Transient outward K$^+$ current reduction prolongs action potentials and promotes afterdepolarisations: a dynamic-clamp study in human and rabbit cardiac atrial myocytes

A. J. Workman[1], G. E. Marshall[1], A. C. Rankin[2], G. L. Smith[1] and J. Dempster[3]

[1] *Institute of Cardiovascular and Medical Sciences, University of Glasgow, Glasgow, UK*
[2] *School of Medicine, University of Glasgow, Glasgow, UK*
[3] *Strathclyde Institute of Pharmacy and Biomedical Sciences, University of Strathclyde, Glasgow, UK*

The Journal of Physiology

Key points

- The shape of the cardiac atrial action potential is influenced by the flow of a transient outward K$^+$ current (I_{TO}) across atrial muscle cell membranes.
- Whether changes in I_{TO} could alter atrial cell action potentials in ways that could affect mechanisms of abnormal heart rhythms (arrhythmias) is unclear, because currently available I_{TO} blocking drugs are non-selective.
- We used the 'dynamic-clamp' technique, for the first time in atrial cells isolated from patients, and from rabbits, to electrically simulate selective changes in I_{TO} during action potential recording.
- We found that I_{TO} decrease prolonged atrial cell action potential duration and, under β-adrenergic-stimulation, provoked abnormal membrane potential oscillations (afterdepolarisations) that were preventable by I_{TO} increase or a β-blocker.
- These results help us better understand the contribution of I_{TO} to atrial cell action potential shape and mechanisms of arrhythmia, with potential implications for both the development and treatment of atrial fibrillation.

Abstract Human atrial transient outward K$^+$ current (I_{TO}) is decreased in a variety of cardiac pathologies, but how I_{TO} reduction alters action potentials (APs) and arrhythmia mechanisms is poorly understood, owing to non-selectivity of I_{TO} blockers. The aim of this study was to investigate effects of selective I_{TO} changes on AP shape and duration (APD), and on afterdepolarisations or abnormal automaticity with β-adrenergic-stimulation, using the dynamic-clamp technique in atrial cells. Human and rabbit atrial cells were isolated by enzymatic dissociation, and electrical activity recorded by whole-cell-patch clamp (35–37°C). Dynamic-clamp-simulated I_{TO} reduction or block slowed AP phase 1 and elevated the plateau, significantly prolonging APD, in both species. In human atrial cells, I_{TO} block (100% I_{TO} subtraction) increased APD$_{50}$ by 31%, APD$_{90}$ by 17%, and APD$_{-61 mV}$ (reflecting cellular effective refractory period) by 22% ($P < 0.05$ for each). Interrupting I_{TO} block at various time points during repolarisation revealed that the APD$_{90}$ increase resulted mainly from plateau-elevation, rather than from phase 1-slowing or any residual I_{TO}. In rabbit atrial cells, partial I_{TO} block ($\sim$40% I_{TO} subtraction) reversibly increased the incidence of cellular arrhythmic depolarisations (CADs; afterdepolarisations and/or abnormal automaticity) in the presence of the β-agonist

isoproterenol (0.1 μM; ISO), from 0% to 64% ($P < 0.05$). ISO-induced CADs were significantly suppressed by dynamic-clamp increase in I_{TO} (~40% I_{TO} addition). ISO+I_{TO} decrease-induced CADs were abolished by β_1-antagonism with atenolol at therapeutic concentration (1 μM). Atrial cell action potential changes from selective I_{TO} modulation, shown for the first time using dynamic-clamp, have the potential to influence reentrant and non-reentrant arrhythmia mechanisms, with implications for both the development and treatment of atrial fibrillation.

Abbreviations 4-AP, 4-aminopyridine; AF, atrial fibrillation; APD, action potential duration; APD_x, action potential duration at x% repolarisation; BCL, basic cycle length; CAD, cellular arrhythmic depolarisation; CHF, congestive heart failure; CICR, Ca^{2+}-induced Ca^{2+} release; CRN, Courtemanche–Ramirez–Nattel; DAD, delayed afterdepolarisation; EAD, early afterdepolarisation; ERP, effective refractory period; h_∞, steady-state inactivation parameter; I_{CaL}, L-type Ca^{2+} current; I_{K1}, inward rectifier K^+ current; I_{KACh}, acetylcholine-activated K^+ current; I_{Kur}, ultra-rapid delayed rectifier K^+ current; $I_{Na/Ca}$, Na^+/Ca^{2+} exchanger current; ISO, isoproterenol; I_{TO}, transient outward K^+ current; I_{TO} G_{max}, peak I_{TO} conductance; LVSD, left ventricular systolic dysfunction; m_∞, steady-state activation parameter; $V_{0.5}$, voltage of half activation or inactivation; V_m, membrane voltage; V_{max}, action potential maximum upstroke velocity; τ_h, inactivation time constant; τ_m, activation time constant.

Introduction

The cardiac transient outward K^+ current (I_{TO}) activates rapidly upon action potential (AP) initiation. Its large magnitude in atrial cells of many species, including human, and in ventricular cells of some rodents contributes to the characteristic spiky AP shape in these cells, with fast early repolarisation (phase 1) and small plateau (Xu *et al.* 1999; Workman *et al.* 2000; Workman *et al.* 2001; Sah *et al.* 2002; Madhvani *et al.* 2011). In such cells, I_{TO} reduction can markedly alter AP shape. For example, in atrial (Xu *et al.* 1999) and ventricular (Sah *et al.* 2002) cells from mice genetically engineered for reduced I_{TO}, the plateau was elevated and AP duration at late (90%) repolarisation (APD_{90}) markedly prolonged. I_{TO} reduction has the potential, therefore, to influence various electrophysiological mechanisms of cardiac arrhythmias. Plateau elevation may cause after-depolarisations or abnormal automaticity, particularly during adrenergic elevation (Workman, 2010), and APD_{90} increase may inhibit reentry (Workman *et al.* 2011).

Atrial fibrillation (AF) is the most common cardiac arrhythmia, and atrial I_{TO} is markedly reduced in chronic AF and in several predisposing pathologies, by electro-physiological remodelling (Le Grand *et al.* 1994; Van Wagoner *et al.* 1997; Nattel *et al.* 2007; Christ *et al.* 2008; Workman *et al.* 2008; Workman *et al.* 2009; Schotten *et al.* 2011; Dobrev *et al.* 2012). Furthermore, some drugs used in the treatment of AF also inhibit I_{TO} (Wang *et al.* 1995; Varro *et al.* 1996; Gross & Castle, 1998; Marshall *et al.* 2012). The rapid activation of this current means that its reduction, by affecting membrane voltage (V_m) early during repolarisation, has knock-on (secondary) effects on other voltage-gated currents, e.g.

L-type Ca^{2+} current (I_{CaL}) and resultant Ca^{2+}-induced Ca^{2+} release (CICR) and Na^+/Ca^{2+}-exchanger current ($I_{Na/Ca}$) (Sah *et al.* 2003) with inevitable complex, species- and pathology-dependent influences on the plateau and APD_{90}.

However, it is unclear what effect I_{TO} reduction has on atrial APs in humans and most other mammals, because of the non-specificity of the best available I_{TO} blocker, 4-aminopyridine (4-AP). This drug additionally blocks ultra-rapid delayed rectifier K^+ current (I_{Kur}) (Wang *et al.* 1993), and although atrial I_{Kur} may be small in some species, e.g. rabbit (Giles & Imaizumi, 1988; Lindblad *et al.* 1996), its large magnitude in human atrium (Wang *et al.* 1993; Van Wagoner *et al.* 1997; Christ *et al.* 2008) necessitates the use of other tools for studying effects of I_{TO} reduction. Mathematical modelling is a powerful alternative, but yielded variable results depending on the algorithm used and intrinsic AP shape, and on constraining electrophysiological parameters (Courtemanche *et al.* 1998; Nygren *et al.* 1998; Zhang *et al.* 2005; Grandi *et al.* 2011; Marshall *et al.* 2012). Moreover, such models can only incorporate known experimental data. The dynamic-clamp technique (Wilders, 2006), however, provides the opportunity to reduce I_{TO} selectively in live atrial cells. A voltage- and time-dependent current based on a mathematical model of I_{TO} is calculated in real-time as a function of the cell's V_m, and injected into the cell with opposite polarity during AP recording, thus cancelling out defined fractions of I_{TO}. Dynamic-clamping has previously been used to alter ventricular I_{TO} or I_{CaL} (Sun & Wang, 2005; Dong *et al.* 2006; Dong *et al.* 2010; Madhvani *et al.* 2011) and a stretch-activated current in rat atrial cells (Wagner *et al.* 2004), but not so far to alter I_{TO} in atrial

cells. No ion current has been studied previously using dynamic-clamping in human atrial cells.

The aim, therefore, was to investigate effects of selective, graded changes in I_{TO} on AP shape and APD, and on after-depolarisations or abnormal automaticity in the presence of β-adrenergic-stimulation, using the dynamic-clamp technique in human and rabbit atrial cells.

Methods

Ethical approval

Procedures and experiments involving human atrial cells were approved by the West of Scotland Research Ethics Service (REC: 99MC002). Written, informed consent was obtained from all patients. The study conformed with the *Declaration of Helsinki*. Procedures and experiments involving rabbit atrial cells (UK Project Licence No. PPL60/40206) were approved by Glasgow University Ethics Review Committee. All procedures and experiments conformed to the principles of UK regulations, as described in Drummond (2009).

Atrial cell isolation

Cells were isolated from rabbit and human atrial tissues, as described previously (Workman *et al.* 2000; Workman *et al.* 2001). Rabbits (New Zealand White, male, age 17.2 ± 1.0 weeks, weight 3.1 ± 0.1 kg; $n = 24$) were humanely killed by intravenous injection of anaesthetic (100 mg kg^{-1} pentobarbital sodium) and removal of the heart, which was retrogradely perfused via the aorta for enzymatic dissociation of left atrial cells (Workman *et al.* 2000). Right atrial appendage tissues were obtained from 14 adult patients (59.4 ± 2.6 years; 13 male/1 female) undergoing cardiac surgery (79%: coronary artery bypass graft; 21%: aortic valve replacement). All patients were in sinus rhythm with no history of AF; 79% had angina, 57% had hypertension, 43% had myocardial infarction, 21% had mild/moderate left ventricular systolic dysfunction (LVSD), 79% had no LVSD. Patients were undergoing treatment with the following cardiac drugs: β-blocker (36%), ACE inhibitor/angiotensin receptor-blocker (36%), Ca^{2+} channel blocker (29%), statin (79%), nitrate (36%), nicorandil (29%). Cells were isolated by the chunk technique (Workman *et al.* 2001), and stored for ≤ 9 h at $\sim 20^\circ$C in a low [Ca^{2+}] solution containing (mM): NaCl (140), KCl (4), CaCl$_2$ (0.18), MgCl$_2$ (1), glucose (11) and Hepes (10); pH 7.4.

Conventional whole-cell-patch clamp technique

Cells were superfused at 35–37°C with the above solution except that [Ca^{2+}] was 1.8 mM. Microelectrodes

(1.5–5 MΩ) contained (mM): potassium aspartate (130), KCl (15), NaCl (10), MgCl$_2$ (1), Hepes (10), EGTA (0.1); pH 7.25. Membrane currents and APs were stimulated and recorded by whole-cell-patch clamp, with an AxoClamp 2B amplifier (Axon Instruments, Union City, CA, USA) and WinWCP or WinEDR software (J. Dempster). I_{TO} was stimulated by voltage-clamping with the activation and inactivation protocols in Fig. 1A and C. Pulse frequency was 0.1 Hz for rabbit, 0.33 Hz for human. I_{TO} amplitude was calculated as peak outward minus end-pulse current, thus avoiding the slowly inactivating I_{Kur} and other slowly or non-inactivating current components that contribute to total outward current in human atrial cells (Christ *et al.* 2008). Extracellular Cd^{2+} (0.2 mM) blocked I_{CaL}. Trains of APs were stimulated at 50–600 beats min^{-1} by current-clamping in bridge mode with 3–5 ms pulses, 1.2–1.5× threshold. Most human atrial cells required a small (0.87 ± 0.19 pA pF^{-1}, $n = 18$) constant hyper-polarising current to gain ~ -80 mV resting V_m, as previously (Le Grand *et al.* 1994; Bénardeau *et al.* 1996; Workman *et al.* 2001).

Dynamic-clamp technique

The dynamic-clamp technique was used in model-clamp configuration (Wilders, 2006) to simulate systematic changes in peak I_{TO} conductance, in rabbit and human live atrial cells. I_{TO} was modelled as a simple Hodgkin–Huxley voltage-activated current based upon an activating parameter, m, and an inactivating parameter, h, using the following equations, based on (Nygren *et al.* 1998).

$$I_{to} = G_{max} mh(V - V_K) \qquad (1)$$

$$\frac{dm}{dt} = \alpha_m m + \beta_m(1 - m), \frac{dh}{dt} = \alpha_h h + \beta_h(1 - h) \quad (2)$$

$$\alpha_m = \frac{m_\infty}{\tau_m}, \beta_m = \frac{1}{\tau_m} - \alpha_m, \alpha_h = \frac{h_\infty}{\tau_h}, \beta_h = \frac{1}{\tau_h} - \alpha_h \quad (3)$$

$$m_\infty = \frac{1}{1 + \exp\left(\dfrac{V + 5.7}{-11.1}\right)},$$
$$\tau_m = 0.84 + 6.6 \exp\left(-\left(\dfrac{V + 29}{25}\right)^2\right) \text{(rabbit)} \qquad (4)$$

$$h_\infty = \frac{1}{1 + \exp\left(\dfrac{V + 34.7}{7.4}\right)},$$
$$\tau_h = 12.5 + 98.5 \exp\left(-\left(\dfrac{V + 90}{70}\right)^2\right) \qquad (5)$$

$$m_\infty = \frac{1}{1 + \exp\left(\dfrac{V - 15}{-7}\right)},$$

$$\tau_m = 0.79 + 36.2 \exp\left(-\left(\frac{V + 40}{45}\right)^2\right) \text{ (human)} \qquad (6)$$

$$h_\infty = \frac{1}{1 + \exp\left(\dfrac{V + 23}{5.3}\right)},$$

$$\tau_h = 8.6 + 162.3 \exp\left(-\left(\frac{V + 32}{27}\right)^2\right) \qquad (7)$$

The voltage dependence of the steady-state activation and inactivation parameters (m_∞, h_∞), activation and inactivation time constant (τ_m, τ_h) and peak I_{TO} conductance (G_{max}) were derived from the average peak current and steady-state activation and inactivation curves, measured in groups of rabbit and human atrial cells (Fig. 1).

The dynamic-clamp was custom-built using an Analog Devices ADuC 7024 analog microcontroller (Analog Devices Inc., Norwood, MA, USA), incorporating a 40 MHz ARM7 microprocessor and 12 bit A/D and D/A converters. The I_{TO} model, executing on the microcontroller, was written in C and the device controlled from a host computer via an RS232 interface. V_m was monitored and dynamic-clamp current output injected into the AxoClamp 2B stimulus current pathway at precisely timed 100 μs intervals.

Statistics

Electrophysiological data are expressed as means ± SEM. Continuous data were compared using two-sided, two-sample paired Student's *t* test; categorical data using a χ^2-test with Yates's correction. $P < 0.05$ was regarded as statistically significant. All statistical and curve fitting analyses were done using Graphpad Prism 5.00 (GraphPad Software Inc., La Jolla, CA, USA).

Results

Comparison of live and simulated atrial I_{TO} characteristics

I_{TO} showed characteristic rapid activation and decay (Fig. 1*Ba* for rabbit; Fig. 1*Bc* for human). A large non-inactivating current was present in human atrial cells, reflecting mainly I_{Kur} (Wang *et al.* 1993). Mean voltage dependence of I_{TO} steady-state activation (Fig. 1*E*) and inactivation (*F*) differed between rabbit and human. I_{TO}

G_{max} was 24.4 nS (0.34 nS pF^{-1}) in rabbit, and 9.9 nS (0.12 nS pF^{-1}) in human atrial cells. The time courses of I_{TO} activation and inactivation were mono-exponential, and mean τ-voltage relationships also differed between species (Fig. 1*G* and *H*). Traces in Fig. 1*B* and *D* (dashed symbols) are dynamic-clamp (i.e. simulated) currents injected into a simple resistor (500 MΩ)–capacitor (33 pF) circuit (Patch-1 model cell, Axon Instruments) during voltage-clamp with the protocols in Fig. 1*A* and *C*. I_{TO} was modelled as a fully inactivating current (Dong *et al.* 2006), so Fig. 1*Bd* and *Dd* do not contain the non-inactivating, I_{Kur} component. There was generally good agreement between live and simulated I_{TO} in both species for I_{TO} waveform, voltage and time dependence curves, and curve fit values (Fig. 1*E–H*). The largest difference was in the steady-state voltage dependence of I_{TO} inactivation in rabbit (Fig. 1*F*), reflected by a 3.9 mV difference in $V_{0.5}$.

Effects of changing I_{TO} by dynamic-clamp on rabbit atrial cell action potentials

Action potentials from rabbit atrial cells had prominent phase 1 repolarisation and low amplitude plateau (Fig. 2*Aa*; control). Partial I_{TO} inhibition, by dynamic-clamp subtraction of a small (5 or 10 nS) peak I_{TO} conductance (Fig. 2*Ab*) slowed phase 1, elevated the plateau, and moderately increased APD (Fig. 2*Aa*). Twenty nanosiemens I_{TO} subtraction, reflecting ∼80% I_{TO} block, markedly slowed phase 1 and elevated the plateau, and prolonged APD, particularly at early-to-mid repolarisation (APD$_{30-50}$). Late repolarisation (e.g. at ≥100 ms; labelled) was also prolonged by I_{TO} subtraction, despite negligible or zero current at ≥100 ms. At approximately full I_{TO} block (25 nS), APs had a prolonged, 'spike & dome' shape (Fig. 2*Aa*). Further (supra-physiological) I_{TO} subtraction (30 nS) produced no extra APD increase. Addition of I_{TO} in this cell (downward deflections in Fig. 2*Ab*) enhanced phase 1 and depressed the plateau (e.g. 20 nS addition in Fig. 2*Aa*), and moderately shortened APD at all levels of repolarisation. Mean data (Fig. 2*B*) revealed a non-linear relationship between I_{TO} and APD, particularly APD$_{20-50}$ due to prominent plateau elevation by I_{TO} subtraction. Action potential maximum upstroke velocity (V_{max}) was unaffected by I_{TO} change (Fig. 2*B*). Full I_{TO} block (24.4 nS I_{TO} subtraction) significantly increased mean APD$_{20-90}$, and APD$_{-64 \text{ mV}}$ (reflecting cellular effective refractory period, ERP; Workman *et al.* 2000), and had no effect on V_{max} (Fig. 2*C*). Absolute APD increase was greatest at APD$_{50}$ (Fig. 2*D*), consistent with the plateau elevation. Nevertheless, APD$_{90}$ and APD$_{-64 \text{ mV}}$ were also increased, by ∼20 ms. Relative (%) APD increase by I_{TO} block was markedly greater at mid than late repolarisation (Fig. 2*E*).
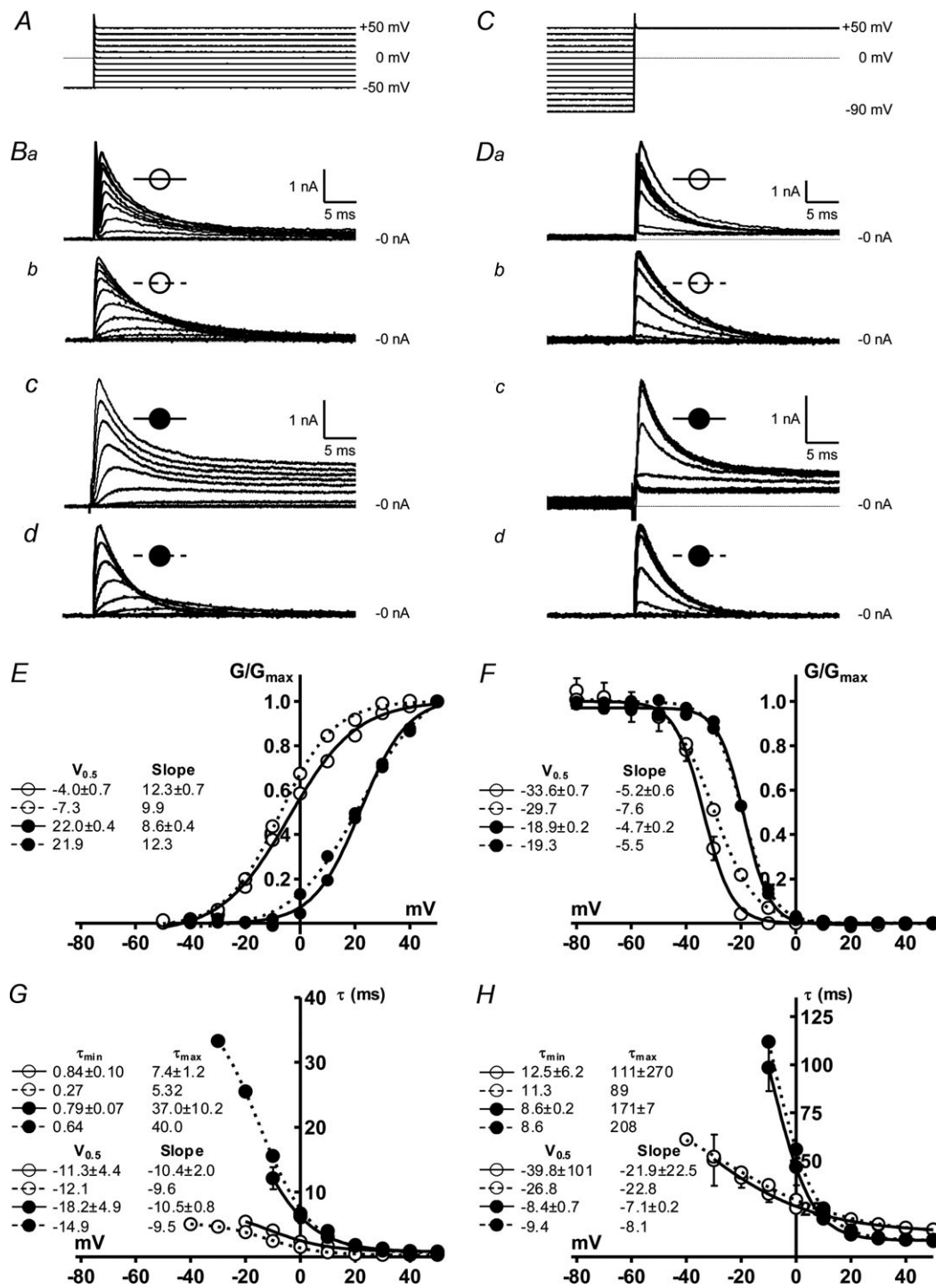
Figure 1. Comparison between live and simulated atrial I_{TO} in rabbit and human

Open symbols: rabbit data; filled symbols: human. Continuous lines: live atrial cell data; dashed lines: current generated by dynamic-clamp I_{TO} models. *A–D*, steady-state voltage dependence: I_{TO} activation, using voltage-clamp protocol shown in *A*, resulting in currents in *Ba–d*; I_{TO} inactivation with protocol shown in *C*, resulting in currents shown in *Da–d*. *E–H*, voltage dependence of I_{TO} activation and inactivation in live atrial cells ($n = 8$–15, 5–6 rabbits; 10–12 cells, 6–7 patients) or from single simulation runs. I_{TO} steady-state activation (*E*) and inactivation (*F*) curves constructed by dividing peak I_{TO} at each voltage by driving force to give conductance, G, and dividing G by G_{max}. I_{TO} activation (*G*) and inactivation (*H*): time constants estimated from exponential functions fitted to activation and inactivation time courses; half-activation and inactivation potentials, $V_{0.5}$, and slopes, minimum and maximum time constants, τ_{min} and τ_{max}, estimated by fitting Boltzmann functions; values shown with corresponding curve labels.

Effects of changing I_{TO} by dynamic-clamp on human atrial cell action potentials

Human atrial cell APs were typically type 3 (low- or no-dome), with prominent phase 1 in control (Fig. 3*Aa*). A 50% inhibition of I_{TO}, by 5 nS dynamic-clamp subtraction (Fig. 3*Ab*), slowed phase 1 and moderately elevated the plateau and prolonged late repolarisation; APD_{70-90} (Fig. 3*Aa*). Full I_{TO} block (10 nS) elevated the plateau further (Fig. 3*Aa*), but less so than in rabbit (Fig. 2*Aa*) and further increased APD. The APD increase at ≥ 150 ms (labelled) occurred despite negligible or zero current at that time. Extra I_{TO} subtraction (15–20 nS; supra-physiological) caused additional increase in late
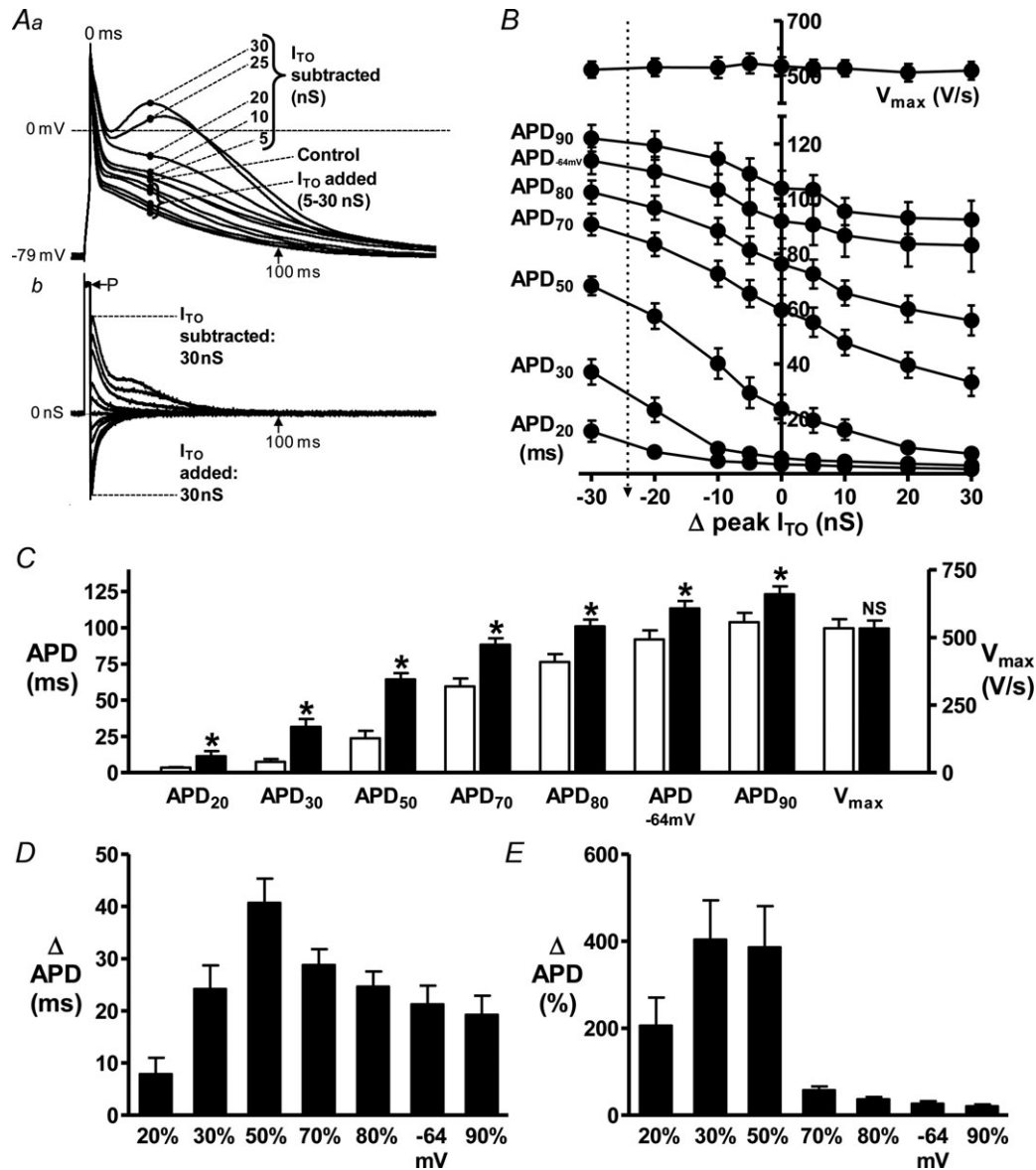

Figure 2. Effects of decreasing and increasing I_{TO} conductance by dynamic-clamp on rabbit atrial cell APs

A, superimposed action potentials (APs; *a*) and corresponding dynamic-clamp (D-C) currents (*b*) recorded from a single representative atrial cell, without D-C (Control), or with D-C subtraction or addition of I_{TO} over a range of peak conductances (labelled). D-C subtracted I_{TO} is +ve, because +ve charge is injected into the cell to compensate for the loss of +ve charge via native I_{TO}. Stimulation rate = 75 beats min^{-1} to permit sufficient time for I_{TO} reactivation (Giles & Imaizumi, 1988; Workman *et al.* 2000). P: current pulse (3 ms, ~1.2× threshold) to stimulate APs. *B*, relationship between I_{TO} conductance (−ve Δ peak I_{TO} = D-C subtraction of I_{TO}) and APD_{20-90}, $APD_{-64\ mV}$ and V_{max}; $n = 16$ cells, 6 rabbits. Vertical arrow indicates 24.4 nS I_{TO} subtraction, reflecting full I_{TO} block. Effect of full I_{TO} block on APDs and V_{max} shown by comparing control (open bars) with 24.4 nS I_{TO} subtraction (filled; *$P < 0.05$ *vs.* control, NS: not significant) (*C*), or as absolute (*D*) or relative (*E*) APD change.

repolarisation and, by contrast with rabbit (Fig. 2A), little further plateau elevation. Dynamic-clamp addition of I_{TO} accelerated phase 1, lowered the plateau and decreased late APD (Fig. 3A). Mean APD changes indicated that within the physiological range of peak I_{TO} conductance (vertical dashed line in Fig. 3B), I_{TO} subtraction lengthened APD, particularly APD_{70-90} and $APD_{-61\,mV}$ (reflecting cellular ERP; Workman *et al.* 2001), and I_{TO} increase had the opposite effects (Fig. 3B). V_{max} was unaltered by I_{TO} change (Fig. 3B). Figure 3C shows that full I_{TO} block

(9.9 nS subtraction) significantly increased APD at each repolarisation level. This was most prominent in absolute terms (Fig. 3D) for APD_{70-90} and $APD_{-61\,mV}$; relative (Fig. 3E) APD increase was similar at each level.

I_{TO} reduction prolongs late repolarisation mainly by elevating action potential plateau

Figure 4Aa and b shows that interrupting the subtraction of I_{TO} late during phase 3 ($\sim APD_{70}$), i.e. when current
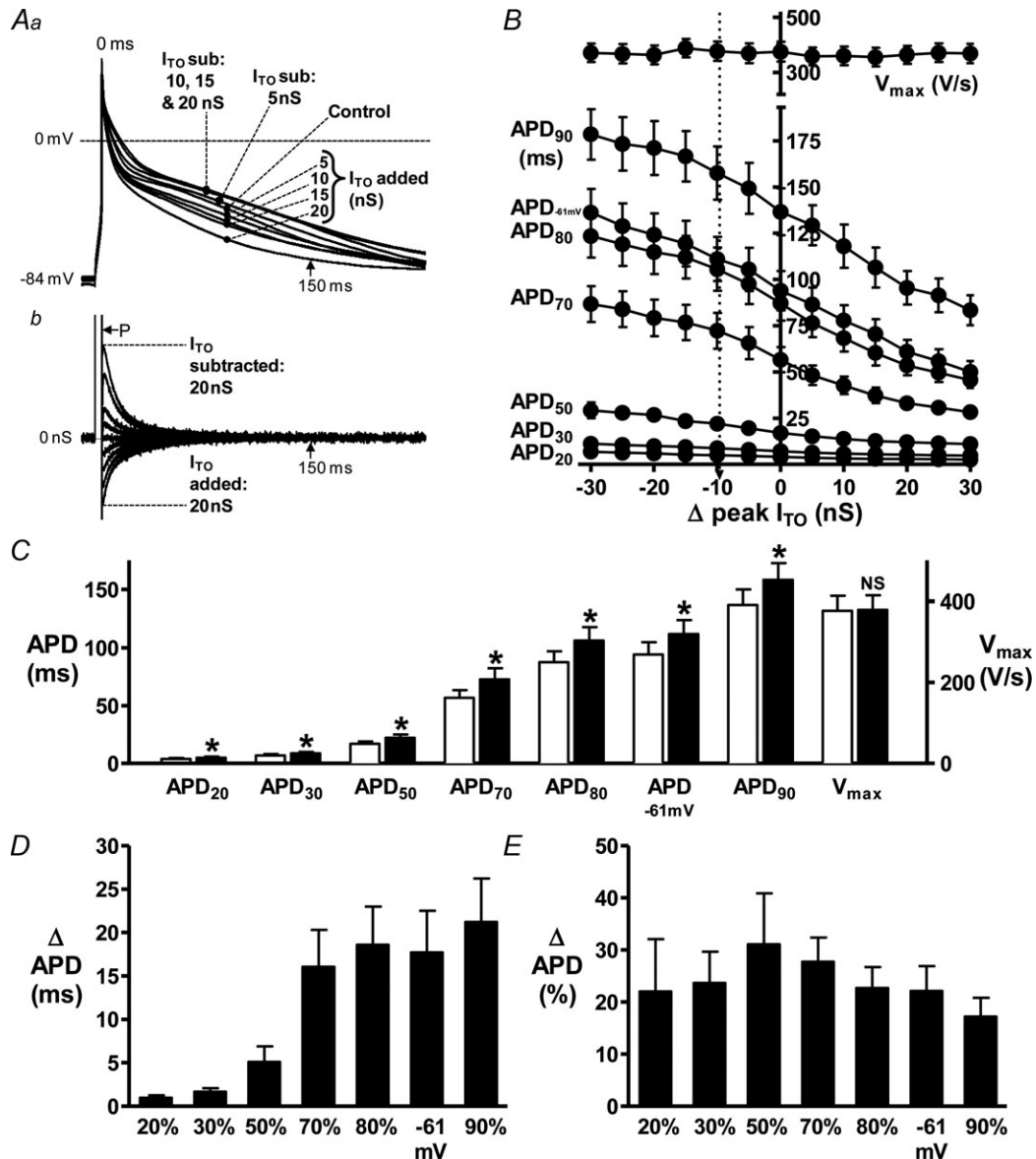

Figure 3. Effects of decreasing and increasing I_{TO} by dynamic-clamp on human atrial cell APs
A, superimposed APs (a) and corresponding D-C currents (b) recorded from a single representative human atrial cell, without D-C (Control), or with D-C subtraction (sub) or addition of I_{TO} over a range of peak conductances. Rate = 75 beats min^{-1}. P: current pulse (5 ms, $\sim$1.5× threshold) to stimulate APs. B, relationship between I_{TO} conductance and APDs and V_{max}; n = 18 cells, 6 patients. Vertical dashed arrow indicates 9.9 nS I_{TO} subtraction, reflecting full I_{TO} block. Effects of full I_{TO} block shown by comparing control (empty bars) with 9.9 nS I_{TO} subtraction (filled; *P < 0.05 vs. control) (C), or as absolute (D) or relative (E) APD change.

was small or zero but APD increase by I_{TO} reduction was large, caused negligible deviation in the course of subsequent repolarisation: compare trace F with I, and see Fig. 4*Aa* inset. This was confirmed by subtracting I from F (Fig. 4*Ac*) and indicated that any residual (non-inactivated) I_{TO} present after APD_{70} contributed little to the APD increase over control (I-C; Fig. 4*Ad*) during that time. When I_{TO} subtraction was interrupted at the end of phase 1 (Fig. 4*B*), i.e. early during repolarisation but when the highest amplitude and a large portion of I_{TO} had already occurred (current leftwards of vertical line in Fig. 4*Bb*), repolarisation rapidly deviated from its course of a slowed phase 1, to follow control: Fig. 4*Ba* and inset. This was confirmed by the small magnitude I-C (Fig. 4*Bd*) and indicated that the marked plateau elevation and APD_{70} increase caused by I_{TO} reduction (F *vs.* C in Fig. 4*Ba*) was not a consequence of the I_{TO} reduction during phase 1. Interrupting I_{TO} subtraction midway through the plateau ($\sim APD_{60}$), i.e. at a point (vertical line in Fig. 4*Ca*) before which I_{TO} reduction had markedly elevated the plateau, caused a moderate deflection in the course of subsequent

repolarisation. The magnitude of F-I rightwards of the vertical line in Fig. 4*Cc* was larger than in 4*Ac*, indicating that a residual I_{TO} block at $\sim APD_{60}$ contributed, albeit to a small degree, to the APD increase during subsequent repolarisation. However, the substantially elevated plateau and prolonged APD observed well beyond the point of interrupting I_{TO} subtraction, i.e. between APD_{60-90} (I-C rightwards of vertical line in Fig. 4*Cd*), showed that the major influence of I_{TO} to prolong APD during that time had occurred earlier, during the plateau and after the end of phase 1, i.e. at around APD_{50-60}.

Production of spontaneous depolarisations in rabbit atrial cells: evidence for DAD component

Spontaneous APs or subthreshold transient depolarisations >3 mV ('cellular arrhythmic depolarisations'; CADs; Redpath *et al.* 2006), which represent afterdepolarisations and/or abnormal automaticity (Redpath *et al.* 2006), occurred during 6 s pauses between AP trains, in rabbit atrial cells (Fig. 5). At BCL 800 ms
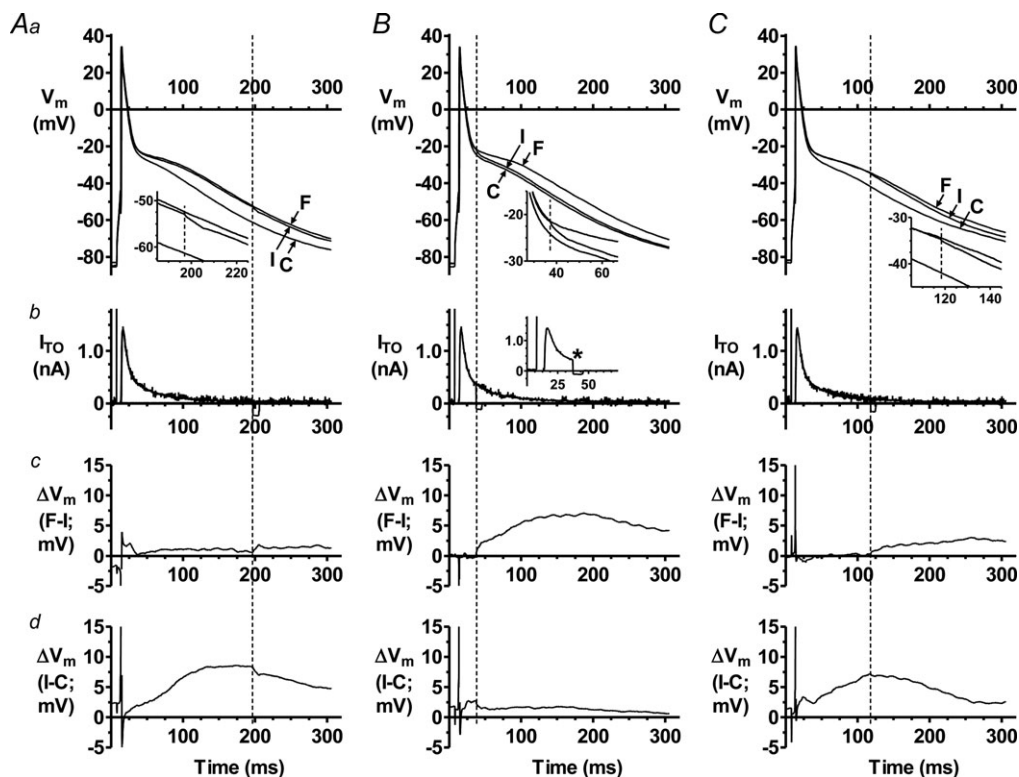

Figure 4. I_{TO} reduction prolongs late repolarisation mainly by elevating AP plateau
Effect on human atrial AP late repolarisation of interrupting D-C subtraction of I_{TO} (by temporarily switching off D-C current injection) during late repolarisation (AP phase 3; *A*), early repolarisation (phase 1; *B*), and mid repolarisation (phase 2; *C*), in a single cell. Rate = 75 beats min^{-1}. Top panels (*a*) show superimposed, representative APs recorded without D-C subtraction of I_{TO} (control: C), or with 9.9 nS I_{TO} subtraction for the full (F) duration of the AP, or with D-C subtraction of I_{TO} interrupted (I) at the point indicated by vertical dashed lines. Insets show magnified portion of APs close to point of interruption. Panels *b* show corresponding superimposed D-C subtraction currents. Inset in *B*, example of non-superimposed D-C-interrupted trace (* Point of interruption). Panels *c* and *d*, subtraction of AP trace I from F, and C from I (as in corresponding top panels).

(used to investigate I_{TO} change on APD), such post-train CAD(s) occurred in 5/12 control cells and in 12/12 cells exposed to the β-receptor agonist isoproterenol (ISO) or ISO+elevated $[Ca^{2+}]_o$ ($P < 0.05$). In a representative cell in which post-train CADs occurred with ISO (Fig. 5A), rapid stimulation (BCL 100 ms) resulted in a high number and frequency of these CADs. Progressive reduction in stimulation rate resulted in fewer post-train CADs, of lower frequency at each rate, and an increase in the time between the last stimulated AP and the first CAD (coupling interval). The lowest rate resulted in a subthreshold post-train CAD. Figure 5B shows a similar coupling interval increase in a different cell. Mean data (Fig. 5C) show a linear relationship between BCL and both coupling interval (panel *a*) and amplitude (*b*) between BCL 100–400 ms, indicating a delayed afterdepolarisation (DAD) component to these CADs.

I_{TO} reduction potentiates β-stimulation-induced CADs in rabbit atrial cells

Effects of dynamic-clamp subtraction of I_{TO} on CADs, in the presence of ISO, were investigated in rabbit atrial cells (Fig. 6). In 24 cells in which no CAD occurred in control (e.g. Fig. 6A, top trace), ISO produced CAD(s) within the pauses between AP trains in 13 cells (e.g. Fig. 6A, lower trace), thus significantly increasing the incidence of post-train CADs (Fig. 6A, bar graph). ISO also elevated the AP plateau, including that of the CAD (Fig. 6A). ISO had no effect on peak I_{TO}: 36.3 ± 4.8 pA pF^{-1} at $+50$ mV in control *vs.* 34.7 ± 4.3 pA pF^{-1} in ISO ($P > 0.05$; $n = 8$ cells, 4 rabbits). In the cells in which ISO did not produce post-train CADs, I_{TO} subtraction (10 nS; ~40% I_{TO} block) during continued ISO elevated the plateau further than ISO alone, and significantly increased the incidence of post-train CADs (Fig. 6B). Furthermore, full I_{TO} block produced post-train CADs in half of the cells in which partial I_{TO} block did not. ISO also produced CADs within AP trains, typically stabilising as rapid, continuously and irregularly firing threshold depolarisations (Fig. 6C). In the 15/24 cells in which these did not occur with ISO, subsequent I_{TO} reduction or block significantly increased the incidence of within-train CADs, again associated with marked plateau-elevation (Fig. 6D).

Production of EADs by I_{TO} reduction plus β-stimulation

Transient, small amplitude depolarisations occurred during the plateau of several APs under I_{TO} subtraction
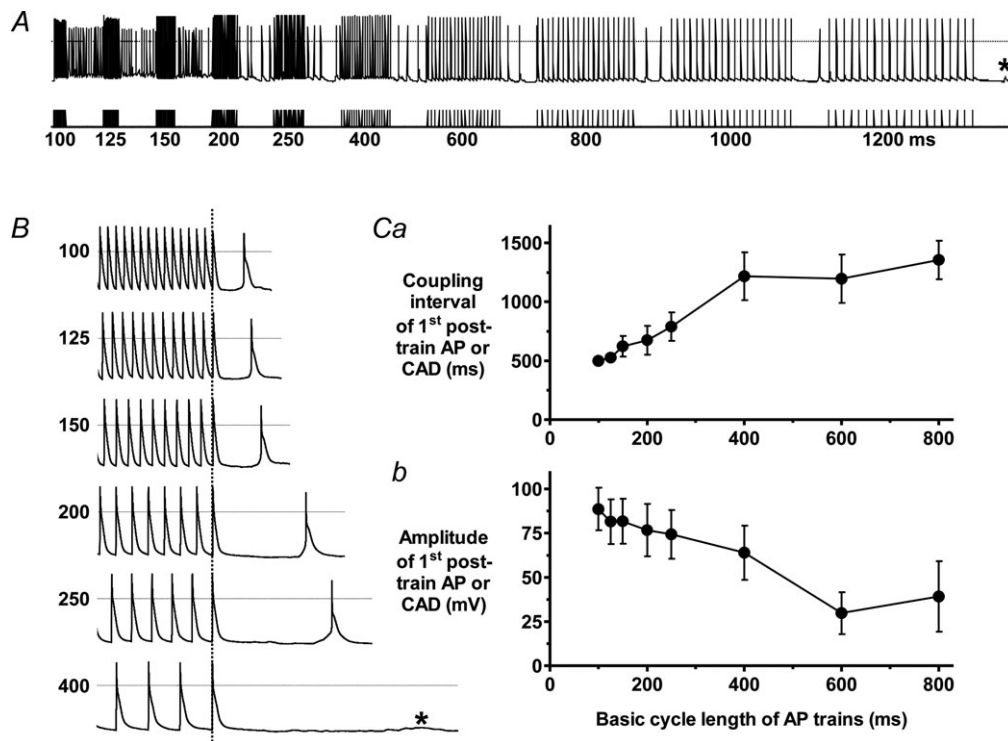

Figure 5. Production of spontaneous depolarisations in rabbit atrial cells: evidence for DAD component
A, APs (upper trace) recorded from a rabbit atrial cell during stimulation with trains of current pulses (lower trace) delivered at BCL shown, in the presence of isoproterenol (ISO) 0.1 μM. *Subthreshold CAD. *B*, APs in a different cell at magnified time scale at short BCLs using same protocol as *A*. *C*, BCL *vs.* mean ($\pm$ SEM) coupling interval (*a*) and amplitude (*b*) of post-train AP or CAD with 0.1 μM ISO or 0.1 μM ISO+3.6 mM $[Ca^{2+}]$. $n = 10$–12 cells, 5 rabbits.

plus ISO, in 1/7 cells (Fig. 7) in which ISO alone did not produce post-train CADs but subsequent 10 nS I_{TO} subtraction did. These plateau phase depolarisations occurred in 0/24 cells treated with ISO alone, appeared ~20 s after I_{TO} subtraction (Fig. 7Ad), persisted during

each AP train (e.g. Fig. 7Ae–h), and disappeared upon ceasing I_{TO} subtraction (Fig. 7Ah). One occurred on the plateau of a post-train CAD (Fig. 7Ag). Over the 2 min period of 10 nS I_{TO} subtraction plus ISO, 117 APs were stimulated in this cell. Of those, 47 (40%) had a plateau
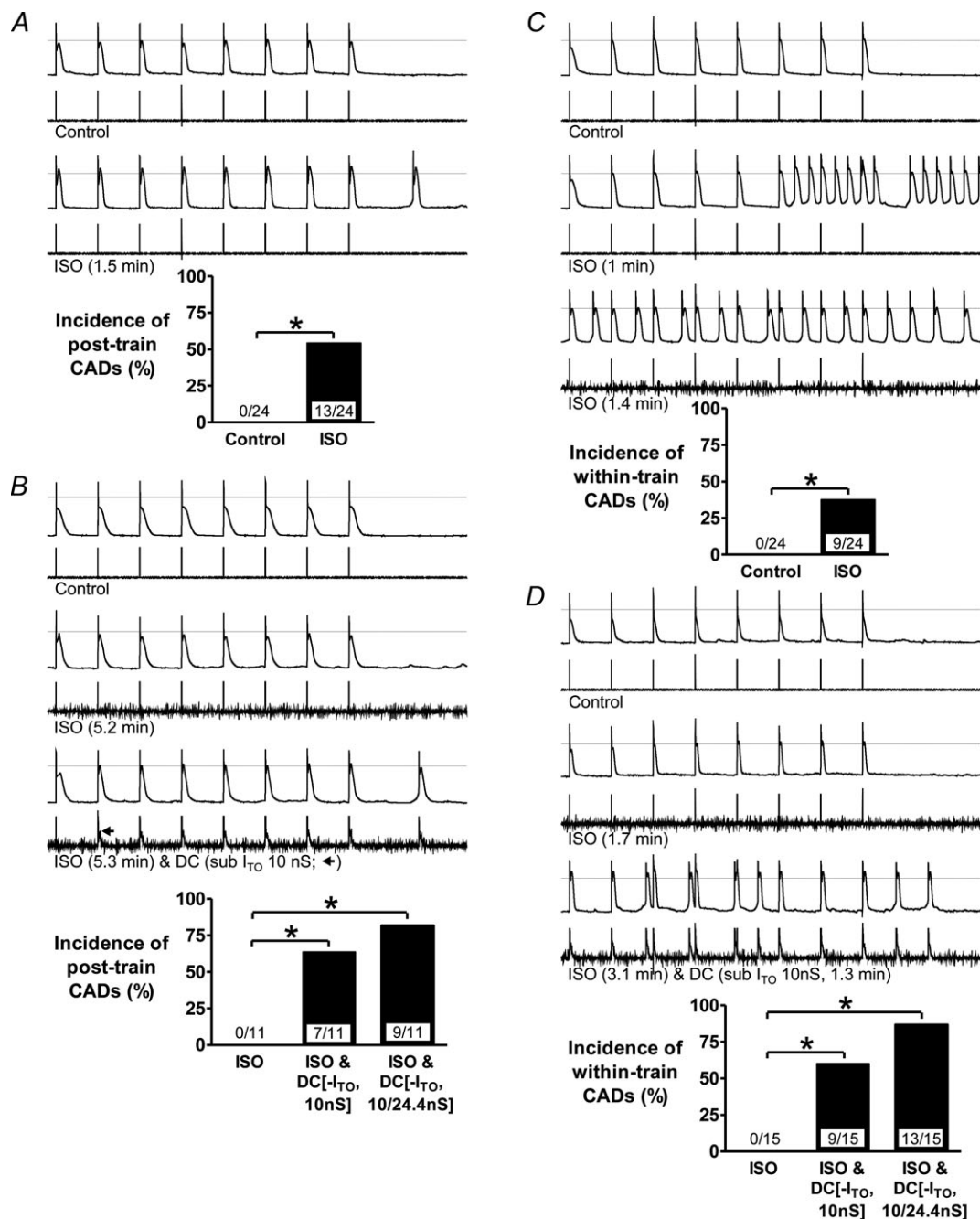

Figure 6. I_{TO} reduction potentiates β-stimulation-induced CADs in rabbit atrial cells
Effects of ISO 0.1 μM with or without D-C subtraction of I_{TO} on the incidence of CADs. Upper traces of trace pairs: AP trains (75 beats min^{-1}) followed by 2 s pauses. Lower traces: corresponding currents: AP stimulus pulses with or without D-C reduction of I_{TO} (of labelled conductance and duration). Bar graphs: incidences of CADs following (post-train) or during (within-train) AP trains; values within bars: cell n ($\leq$7 rabbits), *$P < 0.05$. A, effect of ISO 1.5 min (max. time needed for stable effect on APs and CADs) on post-train CADs, without D-C subtraction of I_{TO}. B, in the cells in which ISO did not produce CADs in A, effects of 10 nS I_{TO} subtraction (3rd trace pair) and/or 24.4 nS I_{TO} subtraction (bar graph) on post-train CADs. C and D, corresponding changes to within-train CADs.

phase depolarisation, and no CAD (threshold or sub-threshold) occurred between stimulated APs (that could suggest DADs or abnormal automaticity), identifying these depolarisations as early afterdepolarisations (EADs). Figure 7*B* shows the EADs as distinct from the AP dome. Full (24.4 nS) I_{TO} subtraction caused a double EAD and a 'late phase' EAD (Fig. 7*Bb*).

Suppression of CADs: by interrupting I_{TO} reduction, by adding I_{TO}, or by β_1-antagonism

Suppression or abolition of CADs that were caused by ISO or concurrent I_{TO} reduction was demonstrated using three interventions (Fig. 8). First, interrupting dynamic-clamp subtraction of I_{TO} in the presence of ISO caused a rapid reduction in the number and frequency of CADs in most cells (e.g. Fig. 8*A*, 2nd trace pair), no further CADs with continued ISO, and accompanying plateau-depression (e.g. Fig. 8*A*, bottom trace pair). Second, increasing I_{TO} (by ∼40%), in cells in which ISO alone produced CADs, typically rapidly and continuously suppressed these CADs, accompanied by plateau depression (e.g. Fig. 8*B*, bottom trace pair), significantly reducing their incidence (Fig. 8*B*, bar graph). Reversibility was assessed in four cells: interrupting I_{TO} addition caused CADs to return in each. Third, β_1-receptor antagonism with atenolol abolished CADs caused by decreased I_{TO} in the presence of ISO (Fig. 8*C*). In each of four cells in which ISO did not produce CADs but subsequent I_{TO} subtraction did (e.g. Fig. 8*C*, top 4 trace pairs) atenolol, in the continued presence of ISO and I_{TO} reduction, abolished these CADs (e.g. Fig. 8*C*, bottom trace pair), significantly decreasing their incidence (Fig. 8*C*, bar graph).
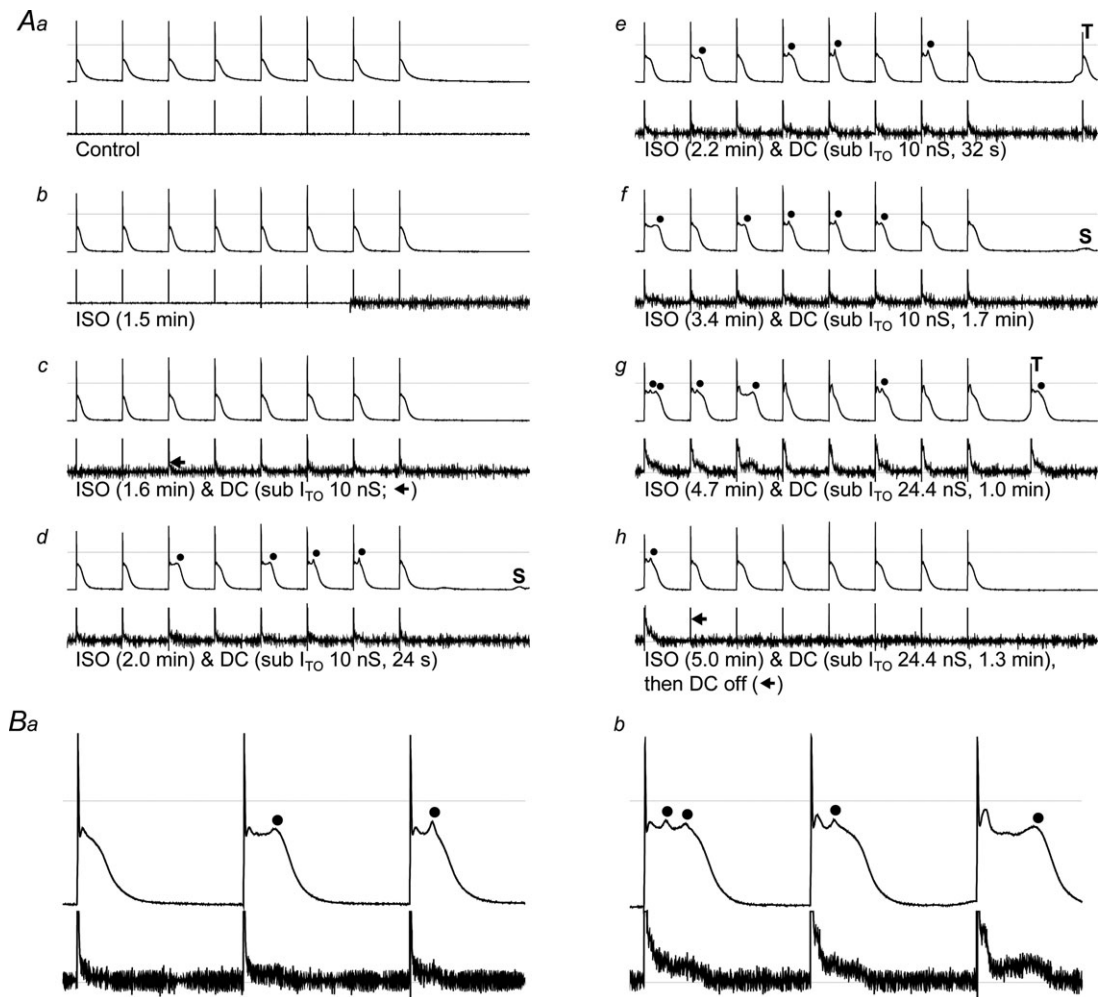

Figure 7. Production of EADs by I_{TO} reduction plus β-stimulation
A, upper traces of trace pairs: AP trains (75 beats min^{-1}) followed by 2 s pauses; lower traces: corresponding currents, recorded in a rabbit atrial cell before (*a*) and after (*b*) ISO 0.1 μM and during subsequent D-C subtraction of I_{TO} (*c–h*). ●: EAD. S, subthreshold CAD; T, threshold CAD. *B*, expanded portions of panel *A* traces: *a*, 4th, 5th and 6th APs from *Ad*; *b*, 1st, 2nd and 3rd APs from *Ag*.
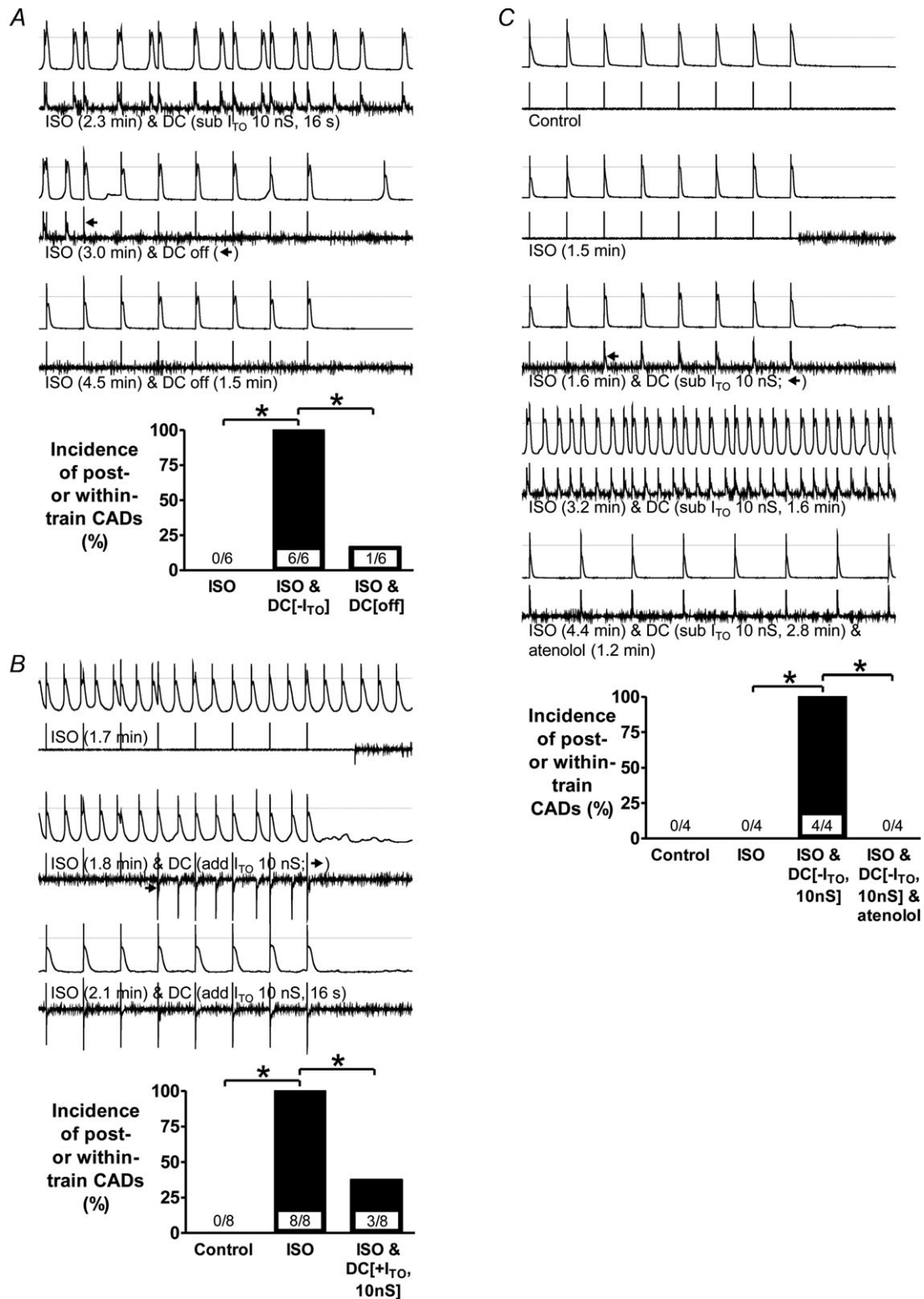
Figure 8. Suppression of CADs by interrupting I_{TO} reduction, by adding I_{TO}, or by β_1-antagonism
Upper traces of trace pairs: AP trains (75 beats min^{-1}) followed by 2 s pauses; lower traces: corresponding currents, recorded in rabbit atrial cells. Bar graphs show incidences of CADs (combined post- and within-train); values within bars: cell *n*, *P < 0.05. *A*, effect of interrupting D-C subtraction of I_{TO} on CADs in cells (3 rabbits) in which ISO did not produce CADs but concurrent D-C subtraction of I_{TO} (10 or 24.4 nS) did. *B*, effect of D-C addition of I_{TO} on CADs in cells (4 rabbits) in which ISO produced CADs. *C*, effect of atenolol (1 μM) on CADs in cells (3 rabbits) in which ISO did not produce CADs but concurrent D-C subtraction of I_{TO} did.

Discussion

The key findings are that selective I_{TO} reduction, simulated in live atrial cells for the first time to our knowledge using dynamic-clamping, elevated the action potential plateau and prolonged late repolarisation (APD_{70-90}) in human and rabbit, and promoted afterdepolarisations or abnormal automaticity under β-adrenergic-stimulation.

Plateau elevation by I_{TO} subtraction was most prominent in rabbit, and terminal repolarisation (APD_{90}) was increased by ∼20% in both species. It was previously unclear what effect I_{TO} reduction would have on human atrial APD_{90}, because the best available I_{TO} blocker, 4-AP, inhibits I_{Kur} at ≥40-fold lower concentration than I_{TO} (Wang *et al.* 1993), human atrial I_{Kur} is large (Wang *et al.* 1993; Van Wagoner *et al.* 1997; Christ *et al.* 2008), and selective I_{Kur} reduction affects human atrial APD_{90} (Wang *et al.* 1993; Wettwer *et al.* 2004). However, I_{Kur} is notoriously difficult to separate completely from I_{TO}, and we cannot exclude the possibility that our I_{TO} model included a component of rapidly inactivating I_{Kur}, as reported by Christ *et al.* (2008). Nevertheless, we were able to exclude the large, slowly inactivating I_{Kur} and other non-inactivating current components (Christ *et al.* 2008) and, therefore, use the dynamic-clamp as a novel intervention to improve our understanding of the contribution of I_{TO} to human atrial cell APD and arrhythmia mechanisms.

Studies of effects of selective I_{Kur} block have shown some similarities to, and important differences from, the present effects of I_{TO} block. Thus, in atrial trabeculae from patients in sinus rhythm, micromolar 4-AP elevated the plateau, but, by contrast with I_{TO} block, here, shortened APD_{90}, probably from secondary increase in delayed rectifier K^+ currents (Wettwer *et al.* 2004). Increase in both plateau and APD_{90}, however, have also been reported in human atrial cells (Wang *et al.* 1993). In canine atrial cells, C9356, an $I_{Kur(d)}$ blocker, increased the plateau, APD_{20} and APD_{50}, but with negligible effect on APD_{90} (Fedida *et al.* 2003). Combined I_{TO}/I_{Kur} block in human atrial cells, with millimolar 4-AP, increased both plateau and APD_{90}, by ∼30% (Workman *et al.* 2001). The novel $I_{Kur}/I_{TO}/I_{KACh}$ blocker, AVE0118, had negligible effect on APD_{90} (Wettwer *et al.* 2004; Schotten *et al.* 2007; Christ *et al.* 2008), but elevated the plateau (Wettwer *et al.* 2004; Schotten *et al.* 2007; Christ *et al.* 2008) and increased systolic $[Ca^{2+}]_i$ and contractility (Schotten *et al.* 2007). Furthermore, Schotten *et al.* (2007) showed, using various AP-clamping techniques, that such change in the AP shape was responsible for this drug's positive inotropic action. Thus, in the absence of AVE0118, atrial cell fractional shortening was markedly increased either by elevating the plateau amplitude or by prolonging its duration (without changing APD_{90}), or indeed by imposing the AP waveform recorded under AVE0118.

Previous dynamic-clamp studies of I_{TO} used ventricular cells, from dog or guinea-pig. In epicardial cells, which have a moderate phase 1 'notch' due to I_{TO}, an I_{TO} subtraction sufficient to eliminate this notch did not affect subsequent repolarisation (Sun & Wang, 2005). In endocardial cells, which had small or no I_{TO} or notch, I_{TO} addition sufficient to produce a notch also lacked effect on repolarisation (Dong *et al.* 2006; Dong *et al.* 2010). However, ventricular AP shape, some ion currents, and $[Ca^{2+}]_i$ handling differ markedly from atrial, including in human (Grandi *et al.* 2011), and the relatively large atrial I_{TO} and phase 1 in human (Grandi *et al.* 2011) and rabbit (Giles & Imaizumi, 1988) are likely to account for the observed relatively strong atrial APD response to I_{TO} decrease.

The magnitude of the human atrial APD_{90} increase with I_{TO} subtraction (i.e. 9% with 50% I_{TO} subtraction) and block (17% with 100% I_{TO} subtraction) is consistent with several mathematical models. Thus, in the Grandi model (Grandi *et al.* 2011), 50 and 100% I_{TO} decrease lengthened APD_{90} by 9 and 19%, respectively. In the Nygren model (Nygren *et al.* 1998), 90% I_{TO} decrease also lengthened APD_{90}, by 18%. By contrast, in the Courtemanche–Ramirez–Nattel (CRN) model (Courtemanche *et al.* 1998), 50 or 90% I_{TO} decrease shortened APD_{90}. Another study, based on the CRN model, also reported APD_{90} shortening (Zhang *et al.* 2005). However, the CRN model generates a type 1 (spike and dome) AP, whereas the present APs and those generated by the other models (Nygren *et al.* 1998; Grandi *et al.* 2011) are type 3. Moreover, modification of the CRN model to generate type 3 s (Marshall *et al.* 2012) reversed the effect of I_{TO} decrease: a 41% decrease lengthened APD_{90} by 9% (Marshall *et al.* 2012), again consistent with present data.

The increased APD_{90} and $APD_{-61\,mV}$ by I_{TO} reduction has implications for atrial reentry. $APD_{-61\,mV}$ estimates cellular ERP, because -61 mV is the mean V_m from which partially refractory APs took off in human atrial cells (Workman *et al.* 2001). Since leading circle reentry wavelength (λ) = ERP × conduction velocity (θ), then increased $APD_{-61\,mV}$, with the unchanged V_{max} (a determinant of θ), has the potential to increase λ and thus inhibit reentry (Workman *et al.* 2011). Furthermore, I_{TO} reduction may terminate spiral wave reentry, by plateau elevation alone, according to a CRN-based mathematical model of human atrial two-dimensional reentry (Pandit *et al.* 2005). Atrial electrophysiological remodelling in chronic AF and predisposing pathologies such as atrial dilatation and LVSD invariably involves I_{TO} reduction (Le Grand *et al.* 1994; Van Wagoner *et al.* 1997; Nattel *et al.* 2007; Christ *et al.* 2008; Workman *et al.* 2008; Workman *et al.* 2009; Schotten *et al.* 2011; Dobrev *et al.* 2012). However, several other currents remodel also, which are likely to have more bearing on atrial ERP than I_{TO},

despite secondary ionic effects of I_{TO} reduction, making the consequences of I_{TO} reduction difficult to predict. For example, increased inward rectifier K^+ current (I_{K1} and I_{KACh}) and altered $[Ca^{2+}]_i$ handling are likely to be the principle mechanisms of ERP-shortening in chronic AF (Dobrev *et al.* 2005; Cha *et al.* 2006; Workman *et al.* 2008; Dobrev *et al.* 2012; Voigt *et al.* 2012). Human atrial ERP increase, by chronic β-blockade (Workman *et al.* 2003), was associated with decreased I_{TO} and I_{K1} (Marshall *et al.* 2012), and mathematical modelling suggested a small contribution from I_{TO} (Marshall *et al.* 2012). It is conceivable that ERP increase by some other drugs used to treat AF, e.g. flecainide, propafenone and amiodarone, could also involve their observed inhibition of I_{TO} (Wang *et al.* 1995; Varro *et al.* 1996; Gross & Castle, 1998), in addition to their recognised effects on other ion currents and $[Ca^{2+}]_i$ handling (Dobrev *et al.* 2012). Since only I_{TO} decrease was detected in patients with LVSD, associated with atrial ERP shortening (Workman *et al.* 2009), the present data indicate that other, as yet unidentified, ionic mechanisms were responsible for the ERP shortening in that study (Workman *et al.* 2009).

Critically timed interruption of I_{TO} subtraction during human atrial repolarisation revealed that the present APD_{90} prolongation was not caused by I_{TO} reduction during phase 1, nor by reduction of any substantial residual I_{TO} flowing during late repolarisation (APD_{70} or beyond), but rather by the effect of I_{TO} reduction between these points, i.e. mid plateau (APD_{50-60}), to elevate the plateau. The mid plateau-to-APD_{90} region is substantially maintained by forward mode (depolarising) $I_{Na/Ca}$ from Ca^{2+} extrusion after CICR: $I_{Na/Ca}$ block with Li^+ approximately halved $APD_{-60\,mV}$ (Bénardeau *et al.* 1996). In mouse ventricular cells, which also have type 3 APs, genetic I_{TO} reduction slowed I_{CaL} inactivation and increased net Ca^{2+} influx via I_{CaL}, and markedly increased systolic $[Ca^{2+}]_i$ (Sah *et al.* 2002). The increased net I_{CaL} in that study is likely to have contributed substantially to the increased $[Ca^{2+}]_i$, but increased reverse-mode $I_{Na/Ca}$ (Ca^{2+} influx) may also contribute, since plateau elevation may shift V_m towards $E_{Na/Ca}$ (Sah *et al.* 2003). Indeed, support for such a contribution from reverse-mode $I_{Na/Ca}$ was provided by the AP-clamp studies in canine atrial cells from Schotten *et al* (2007). They showed that, in control cells, imposing the AP waveform recorded under AVE0118 (a drug which markedly elevated the plateau by inhibiting I_{Kur} and I_{TO}, and increased systolic $[Ca^{2+}]_i$ and contractility) had negligible effect on net Ca^{2+} influx via I_{CaL} despite also increasing contractility, yet inhibition of reverse-mode $I_{Na/Ca}$ (using KBR7943 or elimination of pipette Na^+) abolished this AP-clamp-induced positive inotropic effect (Schotten *et al.* 2007). Irrespective of the mechanism of systolic $[Ca^{2+}]_i$ increase resulting from selective reduction in I_{TO}, a consequent increase in depolarising $I_{Na/Ca}$ is a likely contributory mechanism for

the effect of I_{TO} decrease to prolong APD_{90} in the present study. Furthermore, $I_{Na/Ca}$ is the major current responsible for DADs and abnormal automaticity, especially during adrenergic stimulation, which increases I_{CaL} amplitude, sarcoplasmic reticular Ca^{2+} content, and thus systolic $[Ca^{2+}]_i$ (Workman, 2010).

Afterdepolarisations (DADs and EADs) and abnormal automaticity have complex, partially shared mechanisms of generation and are difficult to distinguish, hence their grouping here as CADs (Redpath *et al.* 2006). We found a DAD component in rabbit atrial cells under β-stimulation, since post-train CADs showed a rate dependence of coupling interval and amplitude characteristic of DADs (Johnson *et al.* 1986). Nevertheless, ISO produced a variety of spontaneous activities, during and after trains, so we did not restrict investigation of I_{TO} change to DADs. ISO was used at E_{max} concentration for I_{CaL} (Redpath *et al.* 2006), and had no effect on I_{TO}. When ISO alone did not produce CADs, it nevertheless elevated the plateau. Subsequent I_{TO} subtraction produced immediate (within 1 beat) further plateau elevation, and CADs followed either within a few beats or after several AP trains, their incidence increasing with strength of I_{TO} subtraction. It is reasonable to suppose that these CADs resulted from the marked plateau elevation from concurrent I_{TO} subtraction and β-stimulation, each of which increases $[Ca^{2+}]_i$ (Sah *et al.* 2002; Dong *et al.* 2010; Workman, 2010), with consequent $[Ca^{2+}]_i$ loading sufficient to produce DADs and/or abnormal automaticity via spontaneous sarcoplasmic reticular Ca^{2+} release and subsequent inward $I_{Na/Ca}$. Furthermore, in one cell, ISO plus I_{TO} subtraction produced EADs, distinguished by their consistent, regular appearance during phase 2, with no DADs or abnormal automaticity. The V_m from which they arose (-25 to -15 mV) centred on 'window I_{CaL}' (where I_{CaL} activation and inactivation curves overlap; -30 to -10 mV in rabbit atrium; Lindblad *et al.* 1996), consistent with a recognised mechanism of EAD generation: APD increase at window I_{CaL} voltages. The contribution of window I_{CaL} to EADs was studied by dynamic-clamping I_{CaL} in rabbit ventricular cells (Madhvani *et al.* 2011). EAD formation was modified by only small changes in I_{CaL} voltage dependence that did not change $[Ca^{2+}]_i$ (Madhvani *et al.* 2011). However, effects of I_{TO} change on window I_{CaL} remain to be studied. Atrial DADs and/or EADs occur in several animal models of congestive heart failure (CHF)-induced AF (Nattel *et al.* 2007; Schotten *et al.* 2011; Dobrev *et al.* 2012). Since these models also feature decreased atrial I_{TO} and increased APD and/or $I_{Na/Ca}$ (Nattel *et al.* 2007; Schotten *et al.* 2011; Dobrev *et al.* 2012), it is conceivable that I_{TO} decrease may contribute to atrial afterdepolarisation formation in CHF. CADs were suppressed, in the present study, by removal of I_{TO} subtraction, or by dynamic-clamp addition of I_{TO}. The associated AP (or CAD) plateau depression in each case

is consistent with suppression of CADs by opposition of $[Ca^{2+}]_i$ loading. CADs were also suppressed by atenolol, used here at therapeutic concentration, $1\,\mu M$ (de Abreu *et al.* 2003), probably involving antagonism of $[Ca^{2+}]_i$ loading produced by β-stimulation of I_{CaL} and CICR (Workman, 2010).

Study limitations

(1) We did not study cells from patients with AF, and since chronic AF remodels atrial ion currents and $[Ca^{2+}]_i$ handling (Schotten *et al.* 2011; Dobrev *et al.* 2012), it may be expected to alter APD responses to I_{TO} change, as shown for some other currents. For example, block of I_{Kur} (Wettwer *et al.* 2004) or $I_{Kur}/I_{TO}/I_{KACh}$ (Wettwer *et al.* 2004; Christ *et al.* 2008) increased APD$_{90}$ in atrial trabeculae from patients with chronic AF, but not sinus rhythm. Chronic AF also increased the propensity for atrial DADs, by increasing diastolic sarcoplasmic reticular Ca^{2+} leak and $I_{Na/Ca}$ (Voigt *et al.* 2012), and so could also alter effects of I_{TO} change on DADs. Whether chronic AF could affect the propensity to EADs, and hence their response to I_{TO} change, is unclear. (2) Whilst the modelled I_{TO} generally conformed well to the live data, with a maximum $V_{0.5}$ discrepancy of $<4\,mV$, an influence of such a difference on the dynamic-clamped AP cannot be excluded. (3) Rabbit and human atrial I_{TO} is carried by different pore-forming α-subunits: Kv1.4 and Kv4.3, respectively (Wang *et al.* 1999), which confer markedly different reactivation kinetics and rate-dependence of I_{TO} between these species. At the stimulation rate (75 beats min^{-1}) and temperature ($35-37^{\circ}C$) used for all the dynamic-clamp experiments, human atrial I_{TO} would reactivate fully between beats, whereas rabbit atrial I_{TO} would be $\sim$50% reactivated (Fermini *et al.* 1992) due to its relatively slow reactivation kinetics. We did not model this slow reactivation, and our rabbit atrial I_{TO} model therefore incorporated more 'human-like' reactivation kinetics than occur *in vivo*. Nevertheless, a subtraction of $\sim$40% of the fully reactivated I_{TO} significantly increased the incidence of afterdepolarisations in the rabbit atrial cells. (4) The holding current required in human (not rabbit) atrial cells to gain $\sim$−80 mV resting V_m, although kept constant in each cell and independent of dynamic-clamp current, is nevertheless recognised to shorten APD and depress the plateau. Such effects could lead to an underestimation of the potential for I_{TO} reduction to produce arrhythmogenic activity in human atrial cells *in vivo*, but an over-estimation of the potential for I_{TO} addition to prevent such activity. (5) Whole-cell-patch clamp uses fixed intra-cellular and extracellular solutions, and the isolated cells also lack electrotonic influence from other cells. (6) The dynamic-clamp was used here to mimic the electrical effects of I_{TO} reduction. However, it is recognised that this technique cannot mimic local $[K^+]$ changes (Wilders, 2006).

In conclusion, changes in atrial cell action potential shape and durations from selective I_{TO} modulation, shown here for the first time using dynamic-clamp, have the potential to influence reentrant and non-reentrant arrhythmia mechanisms, with implications for both the development and treatment of AF.

References

Bénardeau A, Hatem SN, Rücker-Martin C, Le Grand B, Macé L, Dervanian P, Mercadier J-J & Coraboeuf E (1996). Contribution of Na$^+$/Ca^{2+} exchange to action potential of human atrial myocytes. *Am J Physiol Heart Circ Physiol* **271**, H1151–H1161.

Cha TJ, Ehrlich JR, Chartier D, Qi XY, Xiao L & Nattel S (2006). Kir3-based inward rectifier potassium current: potential role in atrial tachycardia remodeling effects on atrial repolarization and arrhythmias. *Circulation* **113**, 1730–1737.

Christ T, Wettwer E, Voigt N, Hala O, Radicke S, Matschke K, Varro A, Dobrev D & Ravens U (2008). Pathology-specific effects of the $I_{Kur}/I_{to}/I_{K,ACh}$ blocker AVE0118 on ion channels in human chronic atrial fibrillation. *Br J Pharmacol* **154**, 1619–1630.

Courtemanche M, Ramirez RJ & Nattel S (1998). Ionic mechanisms underlying human atrial action potential properties: insights from a mathematical model. *Am J Physiol Heart Circ Physiol* **275**, H301–H321.

de Abreu LRP, de Castro SAC & Pedrazzoli J Jr (2003). Atenolol quantification in human plasma by high-performance liquid chromatography: application to bioequivalence study. *AAPS PharmSci* **5**, 1–7.

Dobrev D, Carlsson L & Nattel S (2012). Novel molecular targets for atrial fibrillation therapy. *Nat Rev Drug Discov* **11**, 275–291.

Dobrev D, Friedrich A, Voigt N, Jost N, Wettwer E, Christ T, Knaut M & Ravens U (2005). The G protein-gated potassium current $I_{K,ACh}$ is constitutively active in patients with chronic atrial fibrillation. *Circulation* **112**, 3697–3706.

Dong M, Sun X, Prinz AA & Wang H-S (2006). Effect of simulated I_{to} on guinea pig and canine ventricular action potential morphology. *Am J Physiol Heart Circ Physiol* **291**, H631–H637.

Dong M, Yan S, Chen Y, Niklewski PJ, Sun X, Chenault K & Wang HS (2010). Role of the transient outward current in regulating mechanical properties of canine ventricular myocytes. *J Cardiovasc Electrophysiol* **21**, 697–703.

Drummond GB (2009). Reporting ethical matters in *The Journal of Physiology*: standards and advice. *J Physiol* **587**, 713–719.

Fedida D, Eldstrom J, Hesketh JC, Lamorgese M, Castel L, Steele DF & Van Wagoner DR (2003). Kv1.5 is an important component of repolarizing K$^+$ current in canine atrial myocytes. *Circ Res* **93**, 744–751.

Fermini B, Wang Z, Duan D & Nattel S (1992). Differences in rate dependence of transient outward current in rabbit and human atrium. *Am J Physiol Heart Circ Physiol* **263**, H1747–H1754.

Giles WR & Imaizumi Y (1988). Comparison of potassium currents in rabbit atrial and ventricular cells. *J Physiol* **405**, 123–145.

Grandi E, Pandit SV, Voigt N, Workman AJ, Dobrev D, Jalife J & Bers DM (2011). Human atrial action potential and Ca^{2+} model: sinus rhythm and chronic atrial fibrillation. *Circ Res* **109**, 1055–1066.

Gross GJ & Castle NA (1998). Propafenone inhibition of human atrial myocyte repolarizing currents. *J Mol Cell Cardiol* **30**, 783–793.

Johnson N, Danilo P Jr, Wit AL & Rosen MR (1986). Characteristics of initiation and termination of catecholamine-induced triggered activity in atrial fibers of the coronary sinus. *Circulation* **74**, 1168–1179.

Le Grand B, Hatem S, Deroubaix E, Couetil JP & Coraboeuf E (1994). Depressed transient outward and calcium currents in dilated human atria. *Cardiovasc Res* **28**, 548–556.

Lindblad DS, Murphey CR, Clark JW & Giles WR (1996). A model of the action potential and underlying membrane currents in a rabbit atrial cell. *Am J Physiol Heart Circ Physiol* **271**, H1666–H1696.

Madhvani RV, Xie Y, Pantazis A, Garfinkel A, Qu Z, Weiss JN & Olcese R (2011). Shaping a new Ca^{2+} conductance to suppress early afterdepolarizations in cardiac myocytes. *J Physiol* **589**, 6081–6092.

Marshall GE, Russell JA, Tellez JO, Jhund PS, Currie S, Dempster J, Boyett MR, Kane KA, Rankin AC & Workman AJ (2012). Remodelling of human atrial K^{+} currents but not ion channel expression by chronic β-blockade. *Pflugers Arch* **463**, 537–548.

Nattel S, Maguy A, Le Bouter S & Yeh YH (2007). Arrhythmogenic ion-channel remodeling in the heart: heart failure, myocardial infarction, and atrial fibrillation. *Physiol Rev* **87**, 425–456.

Nygren A, Fiset C, Firek L, Clark JW, Lindblad DS, Clark RB & Giles WR (1998). Mathematical model of an adult human atrial cell: the role of K^{+} currents in repolarization. *Circ Res* **82**, 63–81.

Pandit SV, Berenfeld O, Anumonwo JMB, Zaritski RM, Kneller J, Nattel S & Jalife J (2005). Ionic determinants of functional reentry in a 2-D model of human atrial cells during simulated chronic atrial fibrillation. *Biophys J* **88**, 3806–3821.

Redpath CJ, Rankin AC, Kane KA & Workman AJ (2006). Anti-adrenergic effects of endothelin on human atrial action potentials are potentially anti-arrhythmic. *J Mol Cell Cardiol* **40**, 717–724.

Sah R, Oudit GY, Nguyen TTT, Lim HW, Wickenden AD, Wilson GJ, Molkentin JD & Backx PH (2002). Inhibition of calcineurin and sarcolemmal Ca^{2+} influx protects cardiac morphology and ventricular function in $K_{v}4.2N$ transgenic mice. *Circulation* **105**, 1850–1856.

Sah R, Ramirez RJ, Oudit GY, Gidrewicz D, Trivieri MG, Zobel C & Backx PH (2003). Regulation of cardiac excitation–contraction coupling by action potential repolarization: role of the transient outward potassium current (I_{to}). *J Physiol* **546**, 5–18.

Schotten U, de Haan S, Verheule S, Harks EGA, Frechen D, Bodewig E, Greiser M, Ram R, Maessen J, Kelm M, Allessie M & Van Wagoner DR (2007). Blockade of atrial-specific K^{+}-currents increases atrial but not ventricular contractility by enhancing reverse mode Na^{+}/Ca^{2+}-exchange. *Cardiovasc Res* **73**, 37–47.

Schotten U, Verheule S, Kirchhof P & Goette A (2011). Pathophysiological mechanisms of atrial fibrillation: a translational appraisal. *Physiol Rev* **91**, 265–325.

Sun X & Wang HS (2005). Role of the transient outward current (I_{to}) in shaping canine ventricular action potential – a dynamic clamp study. *J Physiol* **564**, 411–419.

Van Wagoner DR, Pond AL, McCarthy PM, Trimmer JS & Nerbonne JM (1997). Outward K^{+} current densities and Kv1.5 expression are reduced in chronic human atrial fibrillation. *Circ Res* **80**, 772–781.

Varro A, Virag L & Papp JG (1996). Comparison of the chronic and acute effects of amiodarone on the calcium and potassium currents in rabbit isolated cardiac myocytes. *Br J Pharmacol* **117**, 1181–1186.

Voigt N, Li N, Wang Q, Wang W, Trafford AW, Abu-Taha I, Sun Q, Wieland T, Ravens U, Nattel S, Wehrens XHT & Dobrev D (2012). Enhanced sarcoplasmic reticulum Ca^{2+} leak and increased $Na^{+}-Ca^{2+}$ exchanger function underlie delayed afterdepolarizations in patients with chronic atrial fibrillation. *Circulation* **125**, 2059–2070.

Wagner MB, Kumar R, Joyner RW & Wang Y (2004). Induced automaticity in isolated rat atrial cells by incorporation of a stretch-activated conductance. *Pflugers Arch* **447**, 819–829.

Wang Z, Feng J, Shi H, Pond A, Nerbonne JM & Nattel S (1999). Potential molecular basis of different physiological properties of the transient outward K^{+} current in rabbit and human atrial myocytes. *Circ Res* **84**, 551–561.

Wang Z, Fermini B & Nattel S (1993). Sustained depolarisation-induced outward current in human atrial myocytes. Evidence for a novel delayed rectifier K^{+} current similar to Kv1.5 cloned channel currents. *Circ Res* **73**, 1061–1076.

Wang Z, Fermini B & Nattel S (1995). Effects of flecainide, quinidine, and 4-aminopyridine on transient outward and ultrarapid delayed rectifier currents in human atrial myocytes. *J Pharmacol Exp Thera* **272**, 184–196.

Wettwer E, Hala O, Christ T, Heubach JF, Dobrev D, Knaut M, Varro A & Ravens U (2004). Role of I_{Kur} in controlling action potential shape and contractility in the human atrium: influence of chronic atrial fibrillation. *Circulation* **110**, 2299–2306.

Wilders R (2006). Dynamic clamp: a powerful tool in cardiac electrophysiology. *J Physiol* **576**, 349–359.

Workman AJ (2010). Cardiac adrenergic control and atrial fibrillation. *Naunyn Schmiedebergs Arch Pharmacol* **381**, 235–249.

Workman AJ, Kane KA & Rankin AC (2001). The contribution of ionic currents to changes in refractoriness of human atrial myocytes associated with chronic atrial fibrillation. *Cardiovasc Res* **52**, 226–235.

Workman AJ, Kane KA & Rankin AC (2008). Cellular bases for human atrial fibrillation. *Heart Rhythm* **5**, S1–S6.

Workman AJ, Kane KA, Russell JA, Norrie J & Rankin AC (2003). Chronic beta-adrenoceptor blockade and human atrial cell electrophysiology: evidence of pharmacological remodelling. *Cardiovasc Res* **58**, 518–525.

Workman AJ, Kane KA & Rankin AC (2000). Rate-dependency of action potential duration and refractoriness in isolated myocytes from the rabbit AV node and atrium. *J Mol Cell Cardiol* **32**, 1525–1537.

Workman AJ, Pau D, Redpath CJ, Marshall GE, Russell JA, Norrie J, Kane KA & Rankin AC (2009). Atrial cellular electrophysiological changes in patients with ventricular dysfunction may predispose to AF. *Heart Rhythm* **6**, 445–451.

Workman AJ, Smith GL & Rankin AC (2011). Mechanisms of termination and prevention of atrial fibrillation by drug therapy. *Pharmacol Ther* **131**, 221–241.

Xu H, Li H & Nerbonne JM (1999). Elimination of the transient outward current and action potential prolongation in mouse atrial myocytes expressing a dominant negative Kv4 α subunit. *J Physiol* **519**, 11–21.

Zhang H, Garratt CJ, Zhu J & Holden AV (2005). Role of up-regulation of I_{K1} in action potential shortening associated with atrial fibrillation in humans. *Cardiovasc Res* **66**, 493–502.

Author contributions

Acknowledgements